Mechanism of a one-photon two-electron process in photocatalytic hydrogen evolution from ascorbic acid with a cobalt chlorin complex†

Shoko Aoi,[a] Kentaro Mase,[a] Kei Ohkubo[ab] and Shunichi Fukuzumi*[abc]

A one-photon two-electron process was made possible in photocatalytic H_2 evolution from ascorbic acid with a cobalt(II) chlorin complex [Co^{II}(Ch)] *via* electron transfer from ascorbate to the excited state of [$Ru(bpy)_3$]$^{2+}$ followed by electron transfer from [$Ru(bpy)_3$]$^+$ to Co^{II}(Ch) with proton to give the hydride complex, which reacts with proton to produce H_2. [Co^{III}(Ch)]$^+$ was reduced by ascorbate to reproduce Co^{II}(Ch).

Photocatalytic production of hydrogen (H_2) has attracted increasing attention as a clean energy source because of the ever-increasing demand for energy and climate change on our planet.[1] A number of highly efficient hydrogen evolving systems have been developed including homogeneous and heterogeneous photocatalytic systems.[2–13] Two electrons are required to produce H_2 from protons, although one photon generates normally only one electron. A mechanism of photocatalytic production of H_2 was reported to clarify how photoinduced electron transfer of a photosensitiser (a one-electron process) leads to H_2 production (a two-electron process).[14–16] Disproportionation of one-electron reduced species of metal complexes resulted in formation of the two-electron reduced species from which H_2 is formed.[17] Bimolecular reactions of metal(III)–hydride complexes also generate H_2 accompanied by regeneration of metal(II) complexes.[18] In each case, the maximum quantum yield of H_2 production per photon is 50%, because two photons are required to produce two electrons. Thus there has so far been no example for one photon to generate one H_2 molecule.

We report herein photocatalytic H_2 evolution from ascorbic acid ($AscH_2$) with a cobalt(II) chlorin complex [Co^{II}(Ch)] (a chemical structure shown in Scheme 1)[19] in an aqueous acetonitrile solution (H_2O/MeCN), which proceeds *via* a one-photon two-electron process. The photocatalytic mechanism is clarified by nanosecond laser transient absorption spectra and by examining each step in the catalytic cycle independently.

Visible light irradiation of a deaerated (Ar-saturated) H_2O/MeCN solution (1 : 1 v/v) of [$Ru(bpy)_3$]$^{2+}$ (bpy = 2,2′-bipyridine) containing ascorbic acid ($AscH_2$) and ascorbate ($AscH^-$) (E_{ox} = 0.43 V *vs.* SCE) as an electron donor and Co^{II}(Ch) (E_{red} = −0.96 V *vs.* SCE) (Fig. S1 in the ESI†) as a catalyst resulted in H_2 evolution (Fig. 1, black line). When the ratio of $AscH^-$ to $AscH_2$ was changed as fixed total concentrations of $AscH_2$ and $AscH^-$ ([$AscH_2$] + [$AscH^-$] = 1.1 M), the largest H_2 evolution activity was attained with $AscH^-$ (0.30 M) and $AscH_2$ (0.80 M) (Fig. S2 in ESI†). The smaller concentration of $AscH^-$ results in less efficient reductive quenching of the [$Ru(bpy)_3$]$^{2+}$* emission (* denotes the excited state).

[a] Department of Material and Life Science, Graduate School of Engineering, Osaka University, ALCA and SENTAN, Japan Science and Technology Agency (JST), Suita, Osaka 565-0871, Japan. E-mail: fukuzumi@chem.eng.osaka-u.ac.jp; Fax: +81-6-6879-7370

[b] Department of Chemistry and Nano Science, Ewha Womans University, Seoul 120-750, Korea

[c] Faculty of Science and Technology, Meijo University, ALCA and SENTAN, Japan Science and Technology Agency (JST), Nagoya, Aichi 468-8502, Japan

† Electronic supplementary information (ESI) available: Experimental details and cyclic voltammograms (Fig. S1), time courses of H_2 evolution (Fig. S2), emission spectra (Fig. S3 and S5), UV-vis absorption spectra (Fig. S4 and S7) and kinetic data (Fig. S6–S11). See DOI: 10.1039/c5cc05064b
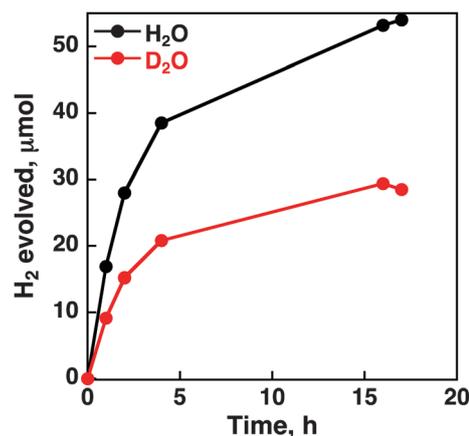
Fig. 1 Time courses of H_2 evolution in the photocatalytic reduction of proton in an Ar-saturated H_2O/MeCN (black) and D_2O/MeCN (red) mixed solution (1 : 1 v/v) containing [Ru^{II}(bpy)$_3$]$^{2+}$ (2.0 mM), $AscH_2$ (0.80 M), AscHNa (0.30 M) and Co^{II}(Ch) (25 μM) under irradiation of visible light (λ > 420 nm) at 298 K.

The quenching efficiency of $[Ru(bpy)_3]^{2+}$* (E_{red} = 0.77 V *vs.* SCE in MeCN)[20] by AscH$^-$ (0.30 M) with AscH$_2$ (0.80 M) was determined to be 95% (Fig. S3 in ESI†). On the other hand, the smaller concentration of AscH$_2$ may retard H$_2$ production due to decreasing the acidity. When H$_2$O was replaced by D$_2$O, D$_2$ and HD were produced without formation of H$_2$. Thus, hydrogen was produced from water and ascorbic acid as electron and proton sources. The observed deuterium kinetic isotope effect (KIE) in Fig. 1 (k_H/k_D = 1.8 in the initial stage) suggests that the Co–H bond cleavage of a cobalt hydride intermediate ($[Co^{III}(H)(Ch)]$) by proton may be the rate-determining step for the photocatalytic H$_2$ evolution (*vide infra*).

The concentration of Co^{II}(Ch) was optimised to be 50 μM for the efficient photocatalytic H$_2$ evolution. The absorption of $[Ru(bpy)_3]^{2+}$ is blocked by the larger concentration of Co^{II}(Ch) (Fig. S4 in ESI†).[21] The quantum yield of the photocatalytic H$_2$ evolution was determined to be 12% using a ferric oxalate actinometer (see the Experimental section in ESI†). This value is similar to the highest value reported for photocatalytic H$_2$ evolution using a cobalt terpyridine complex (Φ = 0.13).[22]

Nanosecond transient absorption spectra of an H$_2$O/MeCN solution of $[Ru(bpy)_3]^{2+}$ with AscH$_2$ and AscH$^-$ are shown in Fig. 2, where appearance of the absorption band at 500 nm due to $[Ru(bpy)_3]^+$ is observed upon the nanosecond laser excitation. Thus, electron transfer from AscH$^-$ to $[Ru(bpy)_3]^{2+}$* occurred to produce AscH$^\bullet$ and $[Ru(bpy)_3]^+$. The rate constant of electron transfer from AscH$^-$ to $[Ru(bpy)_3]^{2+}$* (k_{et}) was determined to be 8.0 × 10^8 M^{-1} s^{-1} from a slope of Stern–Volmer plot (K_{SV} = 3.5 × 10^2 M^{-1}) and the lifetime of $[Ru(bpy)_3]^{2+}$* (0.44 μs in water/MeCN 1:1 v/v) (Fig. S5 in ESI†).[23] The decay rate of absorbance at 500 nm due to $[Ru(bpy)_3]^+$ obeyed the second-order kinetics of bimolecular back electron transfer from $[Ru(bpy)_3]^+$ to AscH$^\bullet$. In the presence of Co^{II}(Ch), the decay of absorbance became much faster because of electron transfer from $[Ru(bpy)_3]^+$ to Co^{II}(Ch) as shown in Fig. 2b. The decay rate constant linearly increased with increasing the concentration of Co^{II}(Ch) (Fig. S6 in ESI†). The rate constant of electron transfer from $[Ru(bpy)_3]^+$ to Co^{II}(Ch) was determined to be 2.5 × 10^9 M^{-1} s^{-1} from the slope of dependence of the first-order decay rate constant on concentration of Co^{II}(Ch) (Fig. S6b in ESI†).

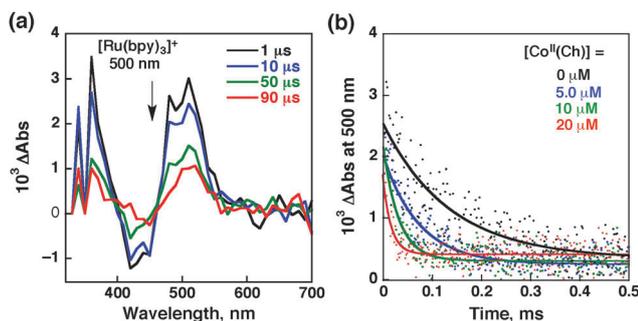Fig. 3 (a) UV-vis absorption spectral changes of $[Co^I(Ch)]^-$ (30 μM) upon addition of CH$_3$COOH (0.30 M) in dearated MeCN at 298 K. The black and blue lines show the spectra taken at 66 ms and 1 s after mixing, respectively. The red line shows UV-vis absorption spectrum of $[Co^I(Ch)]^-$ (15 μM) formed by the electron-transfer reduction of Co^{II}(Ch) (15 μM) with CoCp$_2$* (300 μM) in dearated MeCN at 298 K. (b) Plot of k_{obs} for the rate of formation of $[Co^{III}(Ch)]^+$ *vs.* [CH$_3$COOH].

To examine the reaction of $[Co^I(Ch)]^-$ that is produced by electron transfer from $[Ru(bpy)_3]^+$ to Co^{II}(Ch), $[Co^I(Ch)]^-$ was prepared by the one-electron reduction of Co^{II}(Ch) by deca-methylcobaltocene $[Co(Cp^*)_2]$ in MeCN (Fig. S7 in ESI†). The UV-vis absorption band of $[Co^I(Ch)]^-$ (red line in Fig. 3a; λ_{max} = 510 nm) decreased with increasing absorption band at 660 nm (black line) at 66 ms after addition of acetic acid (CH$_3$COOH) (0.30 M). Then, this absorption band was finally blue shifted to λ_{max} = 652 nm, which is due to $[Co^{III}(Ch)]^+$.[24,25] Thus, $[Co^I(Ch)]^-$ may react with CH$_3$COOH to form the hydride complex ($[Co^{III}(H)(Ch)(CH_3COO)]^-$: λ_{max} = 660 nm), from which H$_2$ was evolved by the reaction with CH$_3$COOH to produce $[Co^{III}(Ch)]^+$. The reaction of $[Co^I(Ch)]^-$ with CH$_3$COOH was monitored by the absorption change at 652 nm due to $[Co^{III}(Ch)]^+$ as shown in Fig. 3, where the rate of the formation of $[Co^{III}(Ch)]^+$ obeyed first-order kinetics (Fig. S8 in ESI†). The first-order rate constant increased with increasing concentration of CH$_3$COOH to approach a constant value (Fig. 3b). Such a saturation behaviour indicates that CH$_3$COOH is not involved in the rate-determining step and that the reaction of $[Co^I(Ch)]^-$ with CH$_3$COOH proceeds *via* formation of the hydride complex ($[Co^{III}(H)(Ch)(CH_3COO)]^-$), followed by the rate-determining heterolytic cleavage of the Co^{III}–H bond. The subsequent reaction of the released hydride ion with CH$_3$COOH to produce H$_2$ and $[Co^{III}(Ch)]^+$ may be fast as compared with the back reaction of the Co^{III}–H bond cleavage (Scheme 1). The kinetic equation for the formation of $[Co^{III}(Ch)]^+$ is given by eqn (1),

Fig. 2 (a) Transient absorption spectra after laser excitation (λ = 450 nm) of $[Ru^{II}(bpy)_3]^{2+}$ (80 μM) in the presence of AscH$_2$ (0.80 M) and AscHNa (0.30 M) in a deaerated H$_2$O/MeCN mixed solution (1:1 v/v) at 298 K. (b) Time profiles of absorbance at 500 nm due to decay of $[Ru(bpy)_3]^+$ in the presence of various concentrations of Co^{II}(Ch) (0–20 μM) in deaerated H$_2$O/MeCN mixed solutions (1:1 v/v) containing $[Ru^{II}(bpy)_3]^{2+}$ (80 μM), AscH$_2$ (0.80 M), AscHNa (0.30 M).

Scheme 1 Mechanism of hydrogen formation by the reaction of $[Co^I(Ch)]^-$ with CH$_3$COOH.

$$d[[Co^{III}(Ch)]^+]/dt = k[[Co^{III}(H)(Ch)(CH_3COO)]^-] \quad (1)$$

where k is the rate constant of the hydrogen evolution. From the equilibrium constant (K), the concentration of a complex between $[Co^I(Ch)]^-$ and CH_3COOH is given by eqn (2), where

$$[[Co^{III}(H)(Ch)(CH_3COO)]^-] = K[CH_3COOH]([[Co^I(Ch)]^-]_0$$
$$- [[Co^{III}(Ch)]^+])/(1 + K[CH_3COOH]) \quad (2)$$

$[[Co^I(Ch)]^-]_0$ is the initial concentration. Eqn (1) is rewritten by eqn (3).

$$d[[Co^{III}(Ch)]^+]/dt = kK[CH_3COOH]([[Co^I(Ch)]^-]_0$$
$$- [[Co^{III}(Ch)]^+])/(1 + K[CH_3COOH]) \quad (3)$$

Under the conditions, the concentration of CH_3COOH is much higher than that of $[Co^I(Ch)]^-$, the k_{obs} value is given by eqn (4). To determine the k value, eqn (4) is rewritten by eqn (5), which predicts

$$k_{obs} = kK[CH_3COOH]/(1 + K[CH_3COOH]) \quad (4)$$

$$k_{obs}^{-1} = 1/kK \cdot [CH_3COOH]^{-1} + 1/k \quad (5)$$

a linear correlation between k_{obs}^{-1} and $[CH_3COOH]^{-1}$ (Fig. S9 in ESI†). The k and K values were determined from the intercept and slope of the linear plot of k_{obs}^{-1} vs. $[CH_3COOH]^{-1}$ to be 5.9 s^{-1} and 7.1 M^{-1}.

When CH_3COOH was replaced by CH_3COOD, the deuterium kinetic isotope effect (KIE) was observed (Fig. S10 in ESI†),[26] indicating that the cleavage of the Co–H bond of $[Co^{III}(H)(Ch)(CH_3COO)]^-$ or O–H bond of CH_3COOH is involved in the rate-determining step of the reaction of $[Co^I(Ch)]^-$ with CH_3COOH. Because CH_3COOH is not involved in the rate-determining step (vide infra), the cleavage of the Co–H bond of $[Co^{III}(H)(Ch)(CH_3COO)]^-$ is the rate-determining step of the reaction of $[Co^I(Ch)]^-$ with CH_3COOH. The KIE value was 1.7 which is virtually the same as observed for the photocatalytic H_2 evolution (KIE = 1.8, Fig. 1), indicating that the heterolytic Co–H bond cleavage of $[Co^{III}(H)(Ch)(CH_3COO)]^-$ is also the rate-determining step in the photocatalytic H_2 evolution.
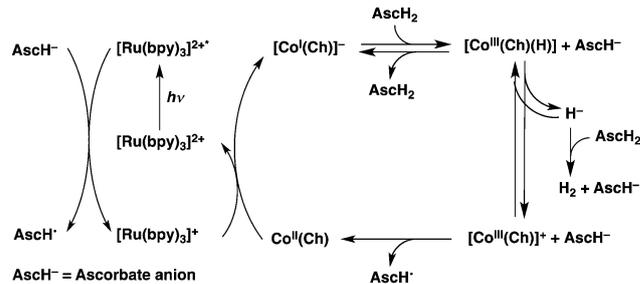
Scheme 2 Mechanism of photocatalytic hydrogen evolution from AscH⁻ and AscH₂ with [Ru(bpy)₃]²⁺ and Co^{II}(Ch).

$[Co^{III}(Ch)]^+$ produced by the reaction of $[Co^{III}(H)(Ch)-(CH_3COO)]^-$ with CH_3COOH is reduced by $AscH^-$ to form $Co^{II}(Ch)$ as shown by stopped-flow measurements in Fig. 4.[27] The rate constant of electron transfer from $AscH^-$ to $[Co^{III}(Ch)]^+$ that was prepared by the one-electron oxidation of $Co^{II}(Ch)$ with $(p\text{-}BrC_6H_4)_3N^{\bullet+}SbCl_6^-$ in $H_2O/MeCN$ was determined to be 1.5×10^3 M^{-1} s^{-1} from the linear dependence of the first-order rate constant on concentration of $AscH^-$ (Fig. S11 in ESI†).

The photocatalytic cycle is summarized in Scheme 2. Photoexcitation of $[Ru(bpy)_3]^{2+}$ resulted in electron transfer from $AscH^-$ to $[Ru(bpy)_3]^{2+*}$ to produce $[Ru(bpy)_3]^+$, followed by electron transfer from $[Ru(bpy)_3]^+$ to $Co^{II}(Ch)$ to produce $[Co^I(Ch)]^-$, which reacts with $AscH_2$ to produce $[Co^{III}(H)(Ch)(AscH)]^-$. Hydrogen is generated by the reaction of $[Co^{III}(H)(Ch)(AscH)]^-$ with $AscH_2$ via the Co–H bond heterolysis to produce $[Co^{III}(Ch)]^+$,[28,29] which is reduced by $AscH^-$ to regenerate $Co^{II}(Ch)$. In such a case, a one-photon two-electron process is made possible, because one photon is required to produce $[Co^I(Ch)]^-$ for H_2 evolution and another electron is provided thermally by $AscH^-$.

In conclusion, $Co^{II}(Ch)$ acts as an efficient catalyst for photocatalytic H_2 evolution from ascorbic acid with $[Ru(bpy)_3]^{2+}$ as a photocatalyst to attain the high quantum yield via a one-photon two-electron process in which the second electron is provided thermally from ascorbic acid.

Notes and references

1 R. A. Kerr and R. F. Service, *Science*, 2005, **309**, 101.
2 X. Song, H. Wen, C. Ma, H. Chen and C. Chen, *New J. Chem.*, 2015, **39**, 1734.
3 K. Kawano, K. Yamauchi and K. Sakai, *Chem. Commun.*, 2014, **50**, 9872.
4 X. Wang, S. Goeb, Z. Ji, N. A. Pogulaichenko and F. N. Castellano, *Inorg. Chem.*, 2011, **50**, 705.
5 L.-Z. Fu, L.-L. Zhou, L.-Z. Tang, Y.-X. Xhang and S.-Z. Zhan, *J. Power Sources*, 2015, **280**, 453.
6 S. Fukuzumi, *Curr. Opin. Chem. Biol.*, 2015, **25**, 18.
7 D. Basu, S. Mazumder, X. Shi, H. Baydoun, J. Niklas, O. Poluektov, H. B. Schlegel and C. N. Verani, *Angew. Chem., Int. Ed.*, 2015, **54**, 2105.
8 A. Call, Z. Codola, F. Acuna-Pares and J. Lloret-Fillol, *Chem. – Eur. J.*, 2014, **20**, 6171.
9 H. Lv, W. Guo, K. Wu, Z. Chen, J. Bacsa, D. G. Musaev, Y. V. Geletii, S. M. Lauinger, T. Lian and C. L. Hill, *J. Am. Chem. Soc.*, 2014, **136**, 14015.
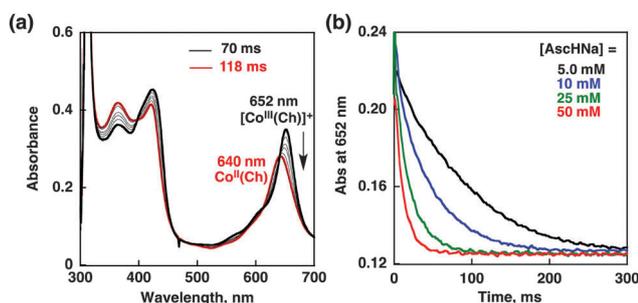

Fig. 4 (a) UV-vis absorption spectral changes in the electron-transfer reduction of $[Co^{III}(Ch)]^+$ (15 μM) with AscHNa (50 mM) in air-saturated $H_2O/MeCN$ mixed solutions (1:1 v/v) at 298 K taken at 70 ms and 118 ms after mixing. (b) Decay time profiles of absorbance at 652 nm due to $[Co^{III}(Ch)]^+$ in the presence of various concentrations of AscHNa in air-saturated $H_2O/MeCN$ mixed solutions (1:1 v/v) at 298 K.

10 L. Chen, G. Chen, C.-F. Leung, S.-M. Yiu, C.-C. Ko, E. Anxolabéhère-Mallart, M. Robert and T.-C. Lau, *ACS Catal.*, 2015, **5**, 356.
11 A. Zarkadoulas, E. Koutsouri, C. Kefalidi and C. A. Mitsopoulou, *Coord. Chem. Rev.*, 2014, **11**, 6.
12 K. Maeda, M. Eguchi and T. Oshima, *Angew. Chem., Int. Ed.*, 2014, **53**, 13164.
13 J. Zhao, Y. Ding, J. Wei, X. Du, Y. Yu and R. Han, *Int. J. Hydrogen Energy*, 2014, **39**, 18908.
14 E. Deponti, A. Luisa, M. Natali, E. Iengo and F. Scandola, *Dalton Trans.*, 2014, **43**, 16345.
15 H. Ozawa and K. Sakai, *Chem. Commun.*, 2011, **47**, 2227.
16 A. Rodenberg, M. Orazietti, B. Probst, C. Bachmann, R. Alberto, K. K. Baldridge and P. Hamm, *Inorg. Chem.*, 2015, **54**, 646.
17 S. Fukuzumi, T. Kobayashi and T. Suenobu, *Angew. Chem., Int. Ed.*, 2011, **50**, 728.
18 J. L. Dempsey, B. S. Brunschwig, J. R. Winkler and H. B. Gray, *Acc. Chem. Res.*, 2009, **42**, 1995.
19 K. Mase, K. Ohkubo and S. Fukuzumi, *J. Am. Chem. Soc.*, 2013, **135**, 2800.
20 J. Yuasa and S. Fukuzumi, *J. Am. Chem. Soc.*, 2006, **128**, 14281.
21 The photocatalytic H_2 evolution in our optimized conditions, the absorption at $\lambda = 450$ nm of $[Ru(bpy)_3]^{2+}$ (2.0 mM, $\varepsilon_{450nm} = 1.4 \times 10^4$ M^{-1} cm^{-1}) is not significantly blocked by that of $Co^{II}(Ch)$ ($Abs_{450nm} = 0.38$; $\varepsilon_{450nm} = 1.8 \times 10^4$ M^{-1} cm^{-1}) under this experimental conditions.
22 C. V. Krishnan and N. Sutin, *J. Am. Chem. Soc.*, 1981, **103**, 2141.
23 The emission lifetime of $[Ru(bpy)_3]^{2+*}$ in water at 298 K was reported to be 0.58 μs; see: J. V. Houten and R. J. Watts, *J. Am. Chem. Soc.*, 1976, **98**, 4853.
24 The spectrum of $[Co^{III}(Ch)]^+$ obtained by the reaction $[Co^I(Ch)]^-$ with CH_3COOH was identical to that of $[Co^{III}(Ch)]^+$ prepared by the electron-transfer oxidation of $Co^{II}(Ch)$ by a one-electron oxidizing reagent of $(p\text{-}BrC_6H_4)_3N^{\bullet+}SbCl_6^-$ ($E_{red} = 1.05$ V *vs.* SCE).[19]
25 $[Co^{III}(Ch)]^+$ or $Co^{III}(H)(Ch)$ species is not re-reduced by large excess of $Co(Cp^\star)_2$, under the present reaction conditions because $Co^{II}(Ch)$ with 20 molar equiv. of $Co(Cp^\star)_2$ is necessary to quantitatively produce $[Co^I(Ch)]^-$ as shown in ESI,† Fig. S7. $Co(Cp^\star)_2$ ($E_{1/2}^{+/0} = -1.47$ V *vs.* SCE) is unstable even in carefully degassed and dehydrated MeCN.
26 The KIE value was determined from the k_{obs} values at $[CH_3COOH] = [CH_3COOD] = 1.0$ M.
27 Neither oxidation of $[Co^{III}(Ch)]^+$ nor O_2 reduction was observed under the basic reaction conditions.
28 S. Mandal, S. Shikano, Y. Yamada, Y.-M. Lee, W. Nam, A. Llobet and S. Fukuzumi, *J. Am. Chem. Soc.*, 2013, **135**, 15294.
29 No Co(II)–H complex is involved in the heterolysis of the Co–H bond as reported in ref. 28.